



# MIT Open Access Articles

## *Light#Controlled, High#Resolution Patterning of Living Engineered Bacteria Onto Textiles, Ceramics, and Plastic*

The MIT Faculty has made this article openly available. **Please share** how this access benefits you. Your story matters.

<b>Citation</b>	Moser, Felix, Tham, Eléonore, González, Lina M., Lu, Timothy K. and Voigt, Christopher A. 2019. "Light#Controlled, High#Resolution Patterning of Living Engineered Bacteria Onto Textiles, Ceramics, and Plastic." <i>Advanced Functional Materials</i> , 29 (30).
<b>As Published</b>	<a href="http://dx.doi.org/10.1002/adfm.201901788">http://dx.doi.org/10.1002/adfm.201901788</a>
<b>Publisher</b>	Wiley
<b>Version</b>	Author's final manuscript
<b>Citable link</b>	<a href="https://hdl.handle.net/1721.1/140977">https://hdl.handle.net/1721.1/140977</a>
<b>Terms of Use</b>	Creative Commons Attribution-Noncommercial-Share Alike
<b>Detailed Terms</b>	<a href="http://creativecommons.org/licenses/by-nc-sa/4.0/">http://creativecommons.org/licenses/by-nc-sa/4.0/</a>

# Light-controlled, high-resolution patterning of living engineered bacteria onto textiles, ceramics, and plastic

Felix Moser<sup>\*1</sup>, Eléonore Tham<sup>\*1,2</sup>, Lina González,<sup>1</sup> Timothy K. Lu<sup>1</sup>, and Christopher A. Voigt<sup>1</sup>

<sup>1</sup> Synthetic Biology Center, Department of Biological Engineering, Massachusetts Institute of Technology, Cambridge, MA 02139, USA

<sup>2</sup> Department of Materials, Massachusetts Institute of Technology, Cambridge, MA 02139, USA

\*These authors contributed equally to this work.

Correspondence and requests for materials should be addressed to C.A.V. (cavoigt@gmail.com)

**Keywords:** genetic circuits, optogenetics, biomaterials, genetic circuits, cellulose, lithography

## Abstract

Living cells can impart materials with advanced functions, such as sense-and-respond, chemical production, toxin remediation, energy generation and storage, self-destruction, and self-healing. Here, we present an approach to use light to pattern *Escherichia coli* onto diverse materials by controlling the expression of curli fibers that anchor the formation of a biofilm. Different colors of light are used to express variants of the structural protein CsgA fused to different peptide tags. By projecting color images onto the material containing bacteria, this system can be used to pattern the growth of composite materials, including layers of protein and gold nanoparticles. This is used to pattern cells onto materials used for 3D printing, plastics (polystyrene), and textiles (cotton). Further, we demonstrate that the adhered cells can respond to sensory information, including small molecules (IPTG and DAPG) and light from LEDs. This work advances the capacity to engineer responsive living materials in which cells provide diverse functionality.

This is the author manuscript accepted for publication and has undergone full peer review but has not been through the copyediting, typesetting, pagination and proofreading process, which may lead to differences between this version and the [Version of Record](#). Please cite this article as [doi: 10.1002/adfm.201901788](https://doi.org/10.1002/adfm.201901788).

## 1. Introduction

Functional materials are increasingly important in applications spanning society, from electronics to textiles. They seek to embed sensing, energy generation and storage, self-repair, and mobility into the material itself. Such functionality is common in materials in nature (*e.g.*, wood and skin) and is provided by cells living in association with a structural scaffold. Cells organize and differentiate in natural materials using complex regulatory networks that control patterns of gene expression as the material grows into a macroscopic three-dimensional form.<sup>[1, 2]</sup> Here, we use patterns of light to control gene expression to promote the adhesion and functionalization of bacteria onto different classes of materials. These bacteria are demonstrated to respond to chemical signals for which it would be difficult to build non-living molecular sensors embedded into the polymer. Further, they can build or recruit materials on command, including nanoparticles and adhesive protein biopolymers, at the micron scale.

Pattern formation in nature often relies on the establishment of chemical gradients that are sensed by cells in order to determine position within a larger structure. Artificial chemical gradients have been established on agar plates, and synthetic genetic sensors and circuits have been used to program patterns of cells.<sup>[3-10]</sup> Establishing reliable gradients, and associated patterns, would be difficult on materials with complex geometries, are flexible, or interact with the diffusible chemical. To this end, light offers a means by which patterns can be precisely projected onto a macroscopic material with fine resolution. A number of synthetic genetic sensors that function in prokaryotes and eukaryotes have been constructed that respond to colored light (including UV and IR) by turning gene expression on or off.<sup>[11-22]</sup> Multiple sensors that respond to different colors have been demonstrated in a single cell, thus different genes can be simultaneously controlled.<sup>[12, 16, 23]</sup> Changes in gene expression have been reported to be induced as quickly as 10 seconds and at 3  $\mu\text{m}$  resolution.<sup>[13, 24]</sup>

Several approaches have been developed to 3D print materials embedded with cells, which enables the mechanical organization of communities.<sup>[25-31]</sup> These are currently limited in scale, in the types of materials in which cells can be embedded, and in the means of keeping cells alive during the printing process. Here, we focus on the patterning of cells onto objects that obtain their form and properties from a non-biological process where construction is not conducive to maintaining living cells. This includes the high-temperature molding of polystyrene, the processing of cotton fibers and weaving into a textile, and the 3D printing of plastics using high-temperatures and UV curing.

Bacteria adhere to solid surfaces by forming a biofilm. This involves the production of an extracellular matrix comprising polysaccharides and protein-based polymers. In *Enterobacteria*, curli fibers are key biofilm components that are secreted and assemble into strong amyloid fibers anchored to the cell wall.<sup>[32]</sup> The genes involved in curli synthesis are encoded in two operons: *csgBAC* and *csgDEFG*. The *csgDEFG* operon is tightly regulated by stress-responsive transcription factors and is induced in nitrogen-poor media at low temperature (30°C).<sup>[33, 34]</sup> CsgD is a transcription factor that stimulates transcription of *csgBAC*. CsgA is secreted into the extracellular medium in a soluble form and the surface-localized CsgB nucleates its polymerization into curli fibers.<sup>[35]</sup> CsgC is thought to prevent premature curli formation in the cytoplasm.<sup>[36]</sup> CsgE, CsgF, and CsgG together comprise the secretion apparatus that selectively transports CsgB and CsgA to the outer membrane of the cell.<sup>[37, 38]</sup> CsgA has been engineered to display peptide tags, which in turn have been used to recruit gold nanoparticles and enzymes to functionalize the fibers.<sup>[39-41]</sup> Such nanoparticles can be further used to quantify curli fiber composition or can make the biofilm conduct electricity.<sup>[5, 42]</sup> These and other functionalities were previously demonstrated by Joshi and coworkers and highlight the versatility of the curli fibers as a substrate for programming chemical functionality.<sup>[39, 40]</sup> Furthermore, this work showed that peptide tags can also increase the affinity of curli-secreting cells to adhere to select materials such as steel.<sup>[39]</sup>

Curli fiber synthesis has been previously placed under the control of genetic sensors and circuits. The control of CsgA by chemical inducers and cell-cell communication signals has been used to change the content of alternative subunits within curli fibers<sup>[5]</sup> and to promote the self-assembly of conductive fibers to form a pressure sensing device.<sup>[43]</sup> Various optogenetic tools have also been used to toggle cell adhesion,<sup>[44]</sup> disrupt biofilms of medical interest,<sup>[45]</sup> and to pattern biofilms at high resolution on a two-dimensional surface.<sup>[46]</sup>

## **2. Results and Discussion**

### **2.1 Optogenetic Control of Biofilm Formation**

We designed a 22-gene genetic system that simultaneously controls the production of three variants of CsgA in response to red, green, and blue light (Figure 1A). This design is based on a multichromatic control system (the "RGB system") reported previously, in which colored light was used to control the expression of different enzymes and CRISPRi sgRNA's that enabled transcription repression of target genes.<sup>[23]</sup> In the RGB system, colored light is perceived by three light sensors based on

phytochromes (red/green) and a LOV domain protein (blue). Each color signal then activates production of one of three different T7 RNAP variants that in turn activate their cognate promoter ( $P_{T3}$ ,  $P_{CGG}$ , or  $P_{K1F}$ ) (Figure 1A). In the system reported here, each T7 promoter controls either wild-type (WT) CsgA or a codon-shuffled variant fused to a different affinity tag (HA or His) (Methods).

To prevent cross-talk between our engineered system and the native curli system, a knockout of the native operons was made in *E. coli* JF1 ( $\Delta csg$ ). The *csgBAC* operon was then placed under control of  $P_{T3}$  (blue light) and recoded variants of CsgA fused to the HA or His affinity tags were placed under the control of  $P_{CGG}$  (green light) and  $P_{K1F}$  (red light), respectively (Figure 1A). Previous work showed that *csgA* fused to these peptide tags can still form curli fibers while retaining the chemical function of the tag.<sup>[39]</sup> Note that the *csgBC* genes were not included with the *csgA* variants because we found that sufficient background expression from  $P_{T3}$  occurred in the absence of blue light. The genes that code for the curli secretion apparatus (*csgE*, *csgF*, and *csgG*) were placed under the control of the IPTG-inducible Ptac promoter. The gene *csgD* was omitted as it encodes a regulatory protein. All *csg* genes were encoded on a pSC101 plasmid (pFM1300), which was co-transformed into *E. coli* JF1  $\Delta csg$  with the plasmids encoding the RGB system (pJFR1, pJFR2, pJFR3).

Following construction, we tested this system for the ability to induce adhesion of cells to the surface of a material in response to colored light. To do this, we diluted an overnight culture of *E. coli* JF1  $\Delta csg$  containing the light-inducible system into liquid LB media and added the diluted culture into a sterile polystyrene petri plate. This plate was placed in a 37°C incubator and a pattern of colored light was projected onto it by a commercial LED projector (Methods). Following incubation for 18 hours, unattached cells were washed away with sterile water, revealing a white film in the shape of the projected pattern. This pattern was strongly stained by crystal violet, indicating that the film was largely composed of cells (Figure 1B). For simplicity, we hereafter refer to these light-induced patterns as "biofilms". We found that the formation of the biofilm patterns was independent of the presence of IPTG, suggesting that leaky expression of the Ptac promoter driving *csgEFG* was sufficient to generate the curli secretion complex. All three colors were able to independently induce the attachment of cells and no adhered cells could be detected on dark sections of the plate. Different colors generated different densities of biofilm (Figure 1B). Testing of different peptide tags fused to *csgA* showed that the resulting curli biofilms varied in their ability to adhere cells (Supplemental Figure S1), suggesting that this is one source of the varying biofilm densities seen in the pattern.

To measure the kinetics of adhesion, a simplified version of the *csg* plasmid was constructed in which only  $P_{T_3}$  (blue light) drives the expression of *csgBAC* and other variants of *csgA* were removed (pFM1019, "Blue Only"). Surprisingly, the biofilm forms after only 3 hours of blue light exposure, despite the culture density still being dilute ( $OD_{600} < 0.05$ ) at that time (Figure 1C and Supplemental Figure S2). In contrast, the native curli system requires 30 hours of growth on nitrogen poor media for biofilm formation.<sup>[32]</sup> The biofilm density could be controlled by varying the intensity of the incident light using the image software (Figure 1C and Supplemental Figure S3). Using this system, we can rapidly create highly intricate patterns of biofilms on polystyrene plates (Supplemental Figure S4).

Next, we tested whether biofilms generated by different colors (i.e. different *CsgA* tag variants) could be differentiated by antibody binding. Biofilms generated by different colors were simultaneously exposed to a mixture of HA- and His-tag specific antibodies that were conjugated to PE-TxRed or FITC fluorophores, respectively. In biofilms formed under blue light (inducing untagged WT *csgA*), no staining is observed by fluorescence microscopy (Figure 1D). When biofilms are formed by red or green light, the biofilms are observed to fluoresce with FITC and PE-TxRed, respectively, confirming labeling of the corresponding antibody. We observed very little nonspecific binding, indicating that the majority of biofilm generated by each color is largely made up of a single curli species (Figure 1D). In addition, we constructed three different strains where each strain responds to a different single color and produces a different tagged *CsgA* (Supplementary Figure S5). These strains could be mixed to generate biofilms in which the curli composition is controlled by the intensity of each color (Supplementary Figure S6). Thus, light-induced control of different curli variants enables control of biofilm composition.

Electron microscopy revealed the organization of cells adhered to the surface. Scanning electron microscopy (SEM) showed that, after 3 hrs of light exposure, clusters of ~10-20 cells are adhered to the surface (Figure 1e). Within these clusters, fibers are visible and appear to hold cells together. These fibers can be imaged at higher resolution with transmission electron microscopy (TEM), which shows a mesh-like network that extends up to several microns away from the cell (Figure 1f).

## 2.2 Biofilms Pattern on Diverse Materials

Peptide tags were also used to incorporate other materials into the biofilm. Ni-NTA conjugated gold nanoparticles were used to label His-tagged curli biofilms (Figure 2a). Furthermore, fusion of CsgA to the A3 peptide enables the nucleation of metallic silver nanoparticles along curli fibers when fibers are incubated with silver nitrate (Figure 2a). We tested the versatility of the untagged (WT) curli biofilm by inducing its formation on a variety of materials, including glass, mica, and 3D-printed plastic polymers such as Vero and VisiJet SL Clear (Figure 2b). The biofilm adhered loosely to some materials (e.g. Vero) and often partially washed off during staining. These materials are present in a variety of contexts, including common labware (glass), electrical insulators and atomic force microscopy substrates (mica), and custom 3D-printed mechanical prototypes (Vero, VisiJet SL Clear).

## 2.3 Biofilm-embedded Cells Respond to Environmental Signals

Controlling the behavior of cells embedded in a material is critical for developing living materials and generating complex biomaterials containing layers of different components. We set out to demonstrate that cells embedded in the biofilm can be further manipulated by light to generate additional function in the biofilm. To do this, we inserted the  $P_{CGG}$  promoter upstream of a GFP gene in a Blue Only system. The resulting strain forms biofilm under blue light and then induces GFP production under green light, generating a pattern of fluorescence within the biofilm (Figure 2C). As a control, an identical red pattern was projected onto on a similar biofilm and no GFP pattern was observed (Figure 2C)

One function that living cells could provide to a material is the ability to sense and respond to changes in the environment. Many genetic sensors, defined as having a signal input and promoter activity output, have been constructed for bacteria.<sup>[47, 48]</sup> Synthetic sensors that respond to chemicals (e.g., TNT),<sup>[49]</sup> toxins,<sup>[50]</sup> temperature,<sup>[51, 52]</sup> pH,<sup>[53]</sup> redox balance,<sup>[54, 55]</sup> metals,<sup>[56]</sup> and other stimuli have been developed. Typically, the response of a sensor is characterized in a planktonic state during exponential growth in a well-mixed and aerated culture.<sup>[57]</sup> Here, we characterized the ability for genetic sensors to function in cells adhered to a surface.

Genetic sensors that respond to a common thiol saccharide inducer (IPTG) and an anti-fungal that is a signature of the soil bacterium *Pseudomonas* (DAPG) were tested in strains after adhesion to a surface. The IPTG sensor is based on the repressor protein LacI, which represses the Ptac promoter (Figure 3a). To image induction on plates, the Ptac promoter is used to drive the production of the LacZ enzyme, which produces a blue color in the presence of its substrate X-gal. Following exposure of cells to a pattern of blue light for 3 hours, cells were adhered in a striped pattern on a polystyrene plate (Figure 3a) (Methods). After the cells are adhered, the plate was washed with sterile water to remove unattached cells. Following washing, we added LB media containing either X-gal and IPTG or just X-gal and incubated the biofilms at 37°C without shaking for 18 hours. Following incubation, the biofilms were again washed twice with water and then imaged. Biofilms to which IPTG had been added were visibly blue in color (Figure 3a). Although IPTG here also drives expression of the csgEFG pathway, this did not appear to interfere with the function of the sensor.

A DAPG-sensing system was similarly constructed and evaluated. For this, the DAPG-sensing PhIF repressor was constitutively expressed from the curli actuator plasmid and its cognate promoter (PphIF) was used to drive expression of GFP. It was necessary to use the red light system here because PhIF is also used to transduce the signal of the blue light system. The red light system contains an empty vector instead of the plasmid expressing blue-light and green-light circuitry. Squares (1 cm x 1 cm) of adhered cells were generated by projecting a pattern of red light into the wells of a 24-well polystyrene plate for 6 hours. Cells were washed and then induced with 25  $\mu$ M DAPG in fresh LB media with antibiotics for 18 hours. By eye, the induced cells can be seen to be producing GFP (Figure 3b). When the adhered cells are imaged with fluorescent microscopy, it can be seen that a fraction of cells are contributing to this fluorescence (Figure 3b). Such heterogeneity has been previously observed during the induction of genetic sensors and circuits in the context of colonies on an agar substrate.<sup>[58]</sup>

## 2.4 Biofilms Integrate Cellular Functions on Wearable Fibers

Adhered cells could also provide a material with the ability to produce a chemical or structural component on demand, for example, the production of a glue when self-repair is required. We chose to demonstrate this in the context of a woven cotton textile, which could be construed as a wearable or as a mesh that scaffolds an architectural or structural material. First, we evaluated whether bacteria could be induced to adhere to cotton using light. To do this, a 2x2 cm square was



cut from a 100% cotton T-shirt and incubated at the bottom of a Petri dish containing LB media with antibiotics and inoculated with cells containing the blue-only system (Figure 4a). After six hours of exposure to blue light, the cotton squares were dried using critical point drying and imaged. SEM of the cotton fabric revealed extensive cell adhesion to cotton squares exposed to blue light whereas very few cells were observed on fabric incubated in the dark (Figure 4b-d). When adhered, most of the fibers were evenly coated with cells. The binding of curli-producing cells here suggests an interaction between curli and cotton fibers. Cotton is primarily composed of plant cellulose fibers but also contains proteins and lipids.<sup>[59]</sup> *E. coli* naturally synthesizes cellulose nanofibers in its biofilms, where it appears to interact with curli to reinforce the biofilm structure and promote adhesion.<sup>[60-63]</sup> These interactions may play a role in the affinity of curli-producing cells on T-shirt cotton here.

We also assessed the ability of cells adhered to cotton to respond to a second light signal. To do this, the strain that could induce GFP in response to green light (Figure 2c) was used to generate biofilms on the cotton squares. After the cells are adhered using blue light, the squares were washed, fresh LB media was added, and 532 nm green light was projected on the cloth for four hours from a fiber with an integrated light-emitting diode (LED).<sup>[64]</sup> Under blue light transillumination, moderate GFP fluorescence was visible from squares exposed to green light (Figure 4e, Supplemental Figure S7). When quantified by imaging software, green light-induced squares showed 65% more GFP fluorescence than uninduced cells (Figure 4f). This difference proved too subtle to allow for GFP pattern generation on T-shirts using an LED projector, despite multiple attempts. Nonetheless, these experiments showed that adhered living cells are able to integrate new spectral properties into wearable textiles in response to an external signal.

The LED fiber we used to illuminate the cotton squares consists of a microscale polycarbonate tubing with a groove on the surface and with embedded wires and LEDs that can be woven into textiles.<sup>[64]</sup> If these fibers were woven into a textile or are embedded as a scaffold in a larger material, then the LEDs could be used to remotely trigger embedded cells. For example, they could induce the production of a chemical, change in color, or produce a material that changes the physical property of the material or causes it to self-repair. Towards this vision, we evaluated whether the LED fiber could induce the localized formation of curli on the fiber in response to blue light. The fiber was submerged in a culture containing cells with the Blue Only wild-type *csqA* system. The LED was turned on for six hours and then the fiber was removed, sectioned, and imaged with SEM. Very few cells were observed on the outside of the fiber and on sections that were 4 cm distant from the LED (Figure 5b-d). However, we observed high numbers of cells in the groove, close

to the LED (Figure 5e-g). These results indicate that LED fibers such as these can be used to recruit biofilm-inducing cells near them and alter their gene expression.

### 3. Conclusion

In this paper, we have engineered cells to form living coatings whose adherence to the outer surface of a variety of materials can be controlled with light. These bacteria remain alive and responsive to chemical and light signals following extensive mechanical washing. The incorporation of such sense-and-respond functionalities into materials, particularly wearable devices and clothing, shows great promise.<sup>[65]</sup> Complementary work has shown the use of bacteria to generate mechanical power, where a sweat-responsive material uses *E. coli* patterned into the fabric to cause it to fold and change airflow in response to humidity.<sup>[66]</sup> Further, to generate nutrients from solar energy, cyanobacteria can be grown in a 3D-printed “gut” that serves as a bioreactor in a wearable that surrounds the waist.<sup>[67, 68]</sup> We previously reported the construction of CsgA fusions to mussel foot proteins to create powerful underwater adhesives.<sup>[69]</sup> Similar designs may be useful to induce adhesion of LED fibers onto fabric or fill a hollow core. Furthermore, using “optogenetic lithography” to repeatedly layer such adhesives with other protein polymers or inorganic layers may enable the production of hierarchically-structured composites that mimic those in nature.<sup>[46, 70]</sup> Given such advances, one can imagine a future in which living cells integrated into materials will enable new applications, such as materials that sense and degrade toxins,<sup>[71, 72]</sup> clothing that regenerates<sup>[73]</sup> or inactivates volatiles in body odor,<sup>[74, 75]</sup> sentinel objects that survey for pathogens,<sup>[76, 77]</sup> nodes that use bacteria to generate power in place of batteries,<sup>[78, 79]</sup> or bandages in which wound healing is managed by consortia.

### 4. Experimental Section

*Strains and media.* The strain *Escherichia coli* JF1 $\Delta$ csg was constructed from the strain *Escherichia coli* JF1 by generating a knockout of all curli associated genes (*csgB*, *csgA*, *csgC*, *csgD*, *csgE*, *csgF*, *csgG*) on the genome using the method of Datsenko and Wanner.<sup>[80]</sup> Briefly, the region containing the *csg* operons (1,101,684..1,105,293 in *Escherichia coli* MG1655) was replaced with a chloramphenicol resistance marker through homologous recombination by lambda red recombinase. This cassette was then removed by FLP recombinase and the genomic locus was sequence verified by PCR and subsequent Sanger sequencing (Quintara). The curli operon was

constructed by amplifying the *csgBAC* and *csgEFG* operons from the genome of *Escherichia coli* MG1655 and assembling them as indicated on a pSC101 plasmid using the Gibson method.<sup>[81]</sup> Recoded *csgA* gene sequences were obtained using the Codon Juggling tool in the GeneDesign software (<http://54.235.254.95/gd/>).<sup>[82]</sup> All cultures were grown in LB broth (BD # 2020-05-31) unless otherwise indicated. Antibiotics were added at the following concentrations to maintain plasmids in all liquid cultures and plates: 50 µg/ml kanamycin (GoldBio #25389-94-0), 100 µg/ml spectinomycin (GoldBio #22189-32-8), 100 µg/ml ampicillin (GoldBio #69-52-3), 35 µg/ml chloramphenicol (AlfaAesar #25-75-7), and 10 µg/ml trimethoprim (Biomedical Inc. #195527).

*Biofilm patterning and staining.* To generate patterns of curli biofilm, fresh cultures were inoculated from single colonies streaked from a glycerol stock frozen at -80°C. Inoculum cultures were grown overnight in 3 ml of LB media at 37°C in 15 ml culture tubes (Falcon #352059) wrapped in aluminum foil to prevent ambient light exposure. The culture was then diluted 1:1000 into 15 ml of fresh LB media containing antibiotics. The diluted culture was then poured into a single 100 mm x 15 mm polystyrene petri dish (Fisher #FB0875713) and placed in a stationary incubator (Boekel Scientific, Model 133000) with a 5 cm hole in top for light projection. As a source of blue light, we used either the PicoPro laser projector (Celluon) or the ST200 LED projector (Aaxa Technologies). As a source of combinations of blue, red and green light, we used only the ST200 LED projector. The measured wavelengths and maximum intensity for the ST200 projector were respectively: 445 nm and 1 mW/cm<sup>2</sup> for blue light, 630 nm and 0.6 mW/cm<sup>2</sup> for red light and 530 nm with 0.7 mW/cm<sup>2</sup> maximal intensity. Cultures were incubated under light as long as needed to form a sufficiently thick layer of curli biofilm (at least 3 hours). Following biofilm formation, the culture media was removed and the plate was washed three times with distilled water with gentle shaking. For photography, the plate was stained with crystal violet by incubating with 5 ml of 2 mM crystal violet (Sigma #548-62-9) for 15 min and was subsequently washed twice with 5 ml of distilled water before drying and imaging.

*Crystal violet staining assay and biofilm quantification.* *Escherichia coli* biofilms were formed on tissue culture treated polystyrene 6 well plates plates (VWR #82050-842) as described above, adjusting the culture volume to 3 ml of LB. Briefly, the plates were incubated for 6 hours at 37°C. After aspiration of planktonic cells, plates were washed three times with phosphate-buffered saline (PBS; VWR # EM-6505) and air-dried. Then, samples were stained with crystal violet (Sigma-

Aldrich, #V5265) by adding 1 mL of 2 mM crystal violet solution to biofilms in each well. The stain was incubated for 15 minutes at room temperature and then washed away three times vigorously with PBS and air dried. Finally, the cell bound crystal violet was dissolved in 1 ml of 30% acetic acid (VWR #97064-482) by incubating for 15 minutes. The absorbance of the resulting solution was measured at 570 nm with a microplate reader (Biotek Synergy H1). Biofilm formation was quantified by measuring the absorbance of crystal violet in samples relative to the absorbance measured under maximum LED projector light intensity for each wavelength (referred to here as % CV binding).

*Antibody staining.* To visualize curli biofilms made with His-tagged *csgA* and HA-tagged *csgA*, we stained these biofilms with His- and HA-specific antibodies conjugated to FITC and PE, respectively (Miltenyi Biotec #130-092-691, #130-092-257). Biofilms were patterned on #1.5 coverslips (Thermo #64-0718) and then blocked overnight in a 3% Bovine Serum Albumin (BSA; Sigma-Aldrich #A9647) solution in PBS (VWR # EM-6505) at 4°C without shaking. The BSA blocking solution was then replaced by antibodies diluted 1:1000 in blocking solution and incubated for 6 hours at 4°C without shaking. Coverslips were washed three times in PBS, sealed to a glass slide, and subsequently imaged with confocal microscopy (Zeiss Laser Scanning Confocal Microscope LSM710).

*Confocal Microscopy.* Antibody-labeled curli biofilms were imaged on a Zeiss Laser Scanning Confocal Microscope LSM710 with 20x air or a 40x oil objective. The PE-TxRed channel used an excitation source by a diode laser at 555 nm and collected emission above 576 nm using an emission filter LP560nm with a secondary dichroic set at 576 nm to remove wavelengths below (Zeiss #1031-350). The FITC channel used an excitation source of 490 nm and collected emission at 490-555 nm (Zeiss #1031-346).

*Transmission Electron Microscopy (TEM).* To assess the formation of curli fibers, we performed transmission electron microscopy on biofilm samples. Biofilm samples were either scratched from the surface of a polystyrene plate or formed directly on TEM grids. Scratched samples were deposited on 200-mesh formvar/carbon coated nickel TEM grids (EMS #FCF200-Ni). The TEM grid was washed twice by placing the grid on top of a 20  $\mu$ l drop of PBS (VWR # EM-6505). The grid was cleaned of PBS by dabbing it lightly on a piece of filter paper (VWR # 28450-048) and was then placed on a 5  $\mu$ l drop of 2% uranyl acetate (VWR #102092-284) for 30 seconds. The grid was then

dabbed clean and placed on a piece of filter paper to dry for at least 1 hour. Transmission Electron Microscopy was performed on a Technai Spirit Transmission Electron Microscope (FEI) operated at 80 kV accelerating voltage at the Whitehead Institute.

*Gold nanoparticle labelling of curli fibers.* For nickel nitrilotriacetic acid gold nanoparticle (NiNTA AuNP) labelling of histidine tags displayed on CsgA, a 200-mesh formvar/carbon coated nickel TEM grid (EMS #FCF200-Ni) was placed face-down for 90 seconds on a 20  $\mu$ l droplet of sample deposited on parafilm. The TEM grid was then rinsed with a 30  $\mu$ l droplet of distilled water for 30 seconds followed by 30 seconds with selective binding buffer (PBS with 0.487M NaCl, 80mM imidazole, and 0.2 v/v% Tween20). Following washing the grid was placed face-down on a 60  $\mu$ l droplet of selective binding buffer containing 10 nM of 5 nm diameter NiNTA-AuNP particles (Nanoprobes #2082). The TEM grid and droplet of parafilm was covered with a petri dish to minimize evaporation and allowed to incubate for 90 minutes. The grid was then washed 5 times with selective binding buffer without NiNTA-AuNP particles, then twice with PBS and twice with ddH<sub>2</sub>O. The thoroughly washed grid was placed face-down on a droplet of filtered 2% uranyl acetate for 30 seconds to negative stain the sample. Excess uranyl acetate was wicked off with filter paper and grid allowed to air dry. All sample preparation steps were done at room temperature.

*Scanning Electron Microscopy (SEM).* Biofilms were grown on 13 mm round Thermanox coverslips (Nunc #174950) that were deposited into 24 well plates and covered in media. Intact biofilms on coverslips were then washed in ethanol-water at 20%, 40%, 60%, 80% and finally 100% to exchange water in the biofilm with ethanol. Samples were placed in a critical point dryer (Tousimus Autosamdri-815) for 8 hours. During this process, the ethanol was replaced with liquid CO<sub>2</sub> and the temperature raised to allow liquid CO<sub>2</sub> to evaporate without distorting the sample morphology. Gold sputtering was performed on the samples with a Quorum Technologies SC 7640 for 60 seconds before imaging. Samples were imaged with a JEOL JSM-6010L scanning electron microscope operated at 10 kV accelerating voltage. Images were obtained in secondary electron imaging (SEI) mode.

*Biofilm induction.* To generate the sensor biofilms, blue light patterns were projected for 6 hours with the ST200 LED projector on a polystyrene Petri dish containing the relevant strain. The

IPTG-sensing strain contained plasmids pJFR1, pJFR2, pFM1019, and pFM1205. The DAPG-sensing strain contained plasmids pJFR1, pJFR3, pFM1019, and pFM725. The green light-sensing strain contained plasmids pJFR1, pJFR2, pJFR3, and pFM1320 (Supplemental Figure S13). Biofilms were washed and then incubated for 18 hours with 10 mL of fresh LB media containing antibiotics as described. For the IPTG-sensing strain, the LB also contained 50 µg/ml X-galactosidase (X-gal), and either no IPTG or 1 mM IPTG. For the DAPG-sensing strain, the LB also contained either no DAPG or 25 µM DAPG. For the green light-sensing strain, the plates were incubated for 4 hours under a new mask projected as either green light (530 nm, 0.7 mW/cm<sup>2</sup>) or as red light (630 nm, 0.6 mW/cm<sup>2</sup>) as a control. The resulting biofilms are then imaged using a Chemidoc imaging system (Bio-Rad #17001401) with Trans-Blue illumination (450-490 nm excitation).

*Patterning biofilms on LED fibers.* Square polycarbonate textile fibers containing either blue or green light-emitting diodes (LED's) producing light at 460 nm or 532 nm, respectively, are connected to a generator. Tungsten wires and LEDs (~100 µm diameter) are embedded in the fibers, where the wires are touching the contact pads of the LED's.<sup>[64]</sup> The LEDs are activated by applying 3 V to the denuded tungsten wires incorporated in the fiber clamped with electrical clips. For the experiments in Figure 4, a green LED fiber was taped on top of the lid of a 6-well plate, directly above a cotton square submersed in LB media containing the strain carrying plasmids pJFR1, pJFR2, pJFR3, and pFM1320. Negative controls were placed in adjacent wells and did not have an LED above the well. The LED was then activated and the culture was incubated at 37°C for 6 hours. For the experiments in Figure 5, blue LED fibers were placed in a Petri dish (Fisher #FB0875713) and submerged in LB containing the strain carrying plasmids pJFR1, pJFR2, pFM1065, and pFM1019. The LED was then activated and the culture was then incubated at 37°C for 6 hours. The LED fiber was then removed, rinsed three times in PBS (VWR # EM-6505) and 0.5 mm sections were cut with a razor blade (VWR #55411-050) at the LED site and 4 cm away. Fiber sections were dried using a critical point dryer (Tousimus Autosamdri-815) and imaged by SEM as described.

*Patterning biofilms on fabric.* Cotton squares of about 2 cm x 2 cm were cut from a 100% cotton t-shirt (Tommy Hilfiger) and incubated at the bottom of 24-well polystyrene plates with a strain containing plasmids pJFR1, pJFR2, pJFR3, and pFM1320. Blue light was projected on the plate with the ST200 LED projector for 6 hours to form blue-light induced curli biofilms on the pieces of fabric. The cotton squares were subsequently washed three times with PBS and incubated in a new

24-well plate with fresh LB media containing antibiotics as described. The plates were either placed directly beneath a green (532 nm, 0.6 mW/cm<sup>2</sup>) LED light source contained in polycarbonate fiber or at least 2 cm away from the fabric for 6 hours. Biofilm-covered cotton pieces from individual experiments were then imaged simultaneously using the Chemidoc (Biorad #17001401) with blue transillumination to detect GFP fluorescence and the cotton fibers were imaged with SEM as described to visualize biofilm formation on the textile fibers. GFP fluorescence quantification on the cotton squares was performed in Adobe Photoshop by calculating the Mean Greyscale Value of a section of each sample's image.

### **Acknowledgements**

We thank Dr. Michael Rein and Prof. Yoel Fink (Advanced Functional Fibers of America, Cambridge, MA) for generously providing LED fibers and assisting with LED fiber experiments. We also thank Prof. Neri Oxman (MIT Media lab), Rachel Soo Hoo Smith, Sunanda Sharma, Christoph Bader, and Dominik Kolb for assistance with biomaterials and providing samples of Vero for patterning. We also thank Frank W. Jarratt for assistance with processing the image of the da Vinci image mask and Irene Pang for assistance with fluorescence quantification in Adobe Photoshop. This work was supported by supported by the Institute for Collaborative Biotechnologies through contract W911NF-09-0001 with the U.S. Army Research Office and through cooperative agreement W911NF-19-2-0026 with the U.S. Army Research Office and the Office of Naval Research Vannevar Bush Faculty Fellowship (formerly NSSEFF) N00014-16-1-2509.

### **Author Contributions**

F.M., E.T., L.G., T.L., and C.A.V designed experiments, analyzed the data, and wrote the manuscript. F.M. designed, built, and tested the genetic systems. E.T. performed immunoassays, LED integration, and SEM. L.G. designed optics hardware and generated biofilm on 3D-printed plastics.

### **Conflict of Interest**

The authors declare no competing financial interest.

## Supporting Information

Supporting information includes:

Supplemental Figures

Plasmid Maps

Supplemental Table S1

## References

- [1] U. G. Wegst, H. Bai, E. Saiz, A. P. Tomsia, R. O. Ritchie, *Nature materials* **2015**, 14, 23.
- [2] P. Q. Nguyen, N. D. Courchesne, A. Duraj-Thatte, P. Praveschotinunt, N. S. Joshi, *Adv Mater* **2018**, 30, e1704847.
- [3] S. Basu, Y. Gerchman, C. H. Collins, F. H. Arnold, R. Weiss, *Nature* **2005**, 434, 1130.
- [4] C. Liu, X. Fu, L. Liu, X. Ren, C. K. Chau, S. Li, L. Xiang, H. Zeng, G. Chen, L. H. Tang, P. Lenz, X. Cui, W. Huang, T. Hwa, J. D. Huang, *Science* **2011**, 334, 238.
- [5] A. Y. Chen, Z. Deng, A. N. Billings, U. O. Seker, M. Y. Lu, R. J. Citorik, B. Zakeri, T. K. Lu, *Nature materials* **2014**, 13, 515.
- [6] D. Karig, K. M. Martini, T. Lu, N. A. DeLateur, N. Goldenfeld, R. Weiss, *Proceedings of the National Academy of Sciences of the United States of America* **2018**, 115, 6572.
- [7] T. S. Moon, E. J. Clarke, E. S. Groban, A. Tamsir, R. M. Clark, M. Eames, T. Kortemme, C. A. Voigt, *Journal of molecular biology* **2011**, 406, 215.
- [8] S. Payne, B. Li, Y. Cao, D. Schaeffer, M. D. Ryser, L. You, *Molecular systems biology* **2013**, 9, 697.
- [9] T. Sohka, R. A. Heins, M. Ostermeier, *J Biol Eng* **2009**, 3, 10.
- [10] J. J. Tabor, H. M. Salis, Z. B. Simpson, A. A. Chevalier, A. Levskaya, E. M. Marcotte, C. A. Voigt, A. D. Ellington, *Cell* **2009**, 137, 1272.
- [11] A. Levskaya, A. A. Chevalier, J. J. Tabor, Z. B. Simpson, L. A. Lavery, M. Levy, E. A. Davidson, A. Scouras, A. D. Ellington, E. M. Marcotte, C. A. Voigt, *Nature* **2005**, 438, 441.
- [12] J. J. Tabor, A. Levskaya, C. A. Voigt, *Journal of molecular biology* **2011**, 405, 315.
- [13] A. Levskaya, O. D. Weiner, W. A. Lim, C. A. Voigt, *Nature* **2009**, 461, 997.



- [14] P. Ramakrishnan, J. J. Tabor, *ACS synthetic biology* **2016**, 5, 733.
- [15] N. T. Ong, E. J. Olson, J. J. Tabor, *ACS synthetic biology* **2018**, 7, 240.
- [16] R. D. Airan, K. R. Thompson, L. E. Fenno, H. Bernstein, K. Deisseroth, *Nature* **2009**, 458, 1025.
- [17] D. Strickland, Y. Lin, E. Wagner, C. M. Hope, J. Zayner, C. Antoniou, T. R. Sosnick, E. L. Weiss, M. Glotzer, *Nature methods* **2012**, 9, 379.
- [18] D. Strickland, K. Moffat, T. R. Sosnick, *Proceedings of the National Academy of Sciences of the United States of America* **2008**, 105, 10709.
- [19] R. Ohlendorf, R. R. Vidavski, A. Eldar, K. Moffat, A. Moglich, *Journal of molecular biology* **2012**, 416, 534.
- [20] T. Han, Q. Chen, H. Liu, *ACS synthetic biology* **2017**, 6, 357.
- [21] A. Baumschlager, S. K. Aoki, M. Khammash, *ACS synthetic biology* **2017**, 6, 2157.
- [22] T. Kim, M. Folcher, M. Doaud-El Baba, M. Fussenegger, *Angew Chem Int Ed Engl* **2015**, 54, 5933.
- [23] J. Fernandez-Rodriguez, F. Moser, M. Song, C. A. Voigt, *Nature chemical biology* **2017**, 13, 706.
- [24] L. B. Motta-Mena, A. Reade, M. J. Mallory, S. Glantz, O. D. Weiner, K. W. Lynch, K. H. Gardner, *Nature chemical biology* **2014**, 10, 196.
- [25] J. Liu, J. Wang, C. Xu, H. Jiang, C. Li, L. Zhang, J. Lin, Z. X. Shen, *Adv Sci (Weinh)* **2018**, 5, 1700322.
- [26] J. N. Hanson Shepherd, S. T. Parker, R. F. Shepherd, M. U. Gillette, J. A. Lewis, R. G. Nuzzo, *Adv Funct Mater* **2011**, 21, 47.
- [27] D. B. Kolesky, R. L. Truby, A. S. Gladman, T. A. Busbee, K. A. Homan, J. A. Lewis, *Advanced materials* **2014**, 26, 3124.
- [28] A. Park, B. Wu, L. G. Griffith, *J Biomater Sci Polym Ed* **1998**, 9, 89.
- [29] B. A. E. Lehner, D. T. Schmieden, A. S. Meyer, *ACS synthetic biology* **2017**, 6, 1124.
- [30] J. Huang, S. Liu, C. Zhang, X. Wang, J. Pu, F. Ba, S. Xue, H. Ye, T. Zhao, K. Li, Y. Wang, J. Zhang, L. Wang, C. Fan, T. K. Lu, C. Zhong, *Nature chemical biology* **2019**, 15, 34.
- [31] D. T. Schmieden, S. J. Basalo Vazquez, H. Sanguesa, M. van der Does, T. Idema, A. S. Meyer, *ACS synthetic biology* **2018**, 7, 1328.
- [32] M. R. Chapman, L. S. Robinson, J. S. Pinkner, R. Roth, J. Heuser, M. Hammar, S. Normark, S. J. Hultgren, *Science* **2002**, 295, 851.
- [33] D. O. Serra, A. M. Richter, G. Klauk, F. Mika, R. Hengge, *mBio* **2013**, 4, e00103.

- [34] X. Zogaj, W. Bokranz, M. Nimtz, U. Romling, *Infect Immun* **2003**, 71, 4151.
- [35] M. M. Barnhart, M. R. Chapman, *Annu Rev Microbiol* **2006**, 60, 131.
- [36] M. L. Evans, E. Chorell, J. D. Taylor, J. Aden, A. Gotheson, F. Li, M. Koch, L. Sefer, S. J. Matthews, P. Wittung-Stafshede, F. Almqvist, M. R. Chapman, *Mol Cell* **2015**, 57, 445.
- [37] M. L. Evans, M. R. Chapman, *Biochim Biophys Acta* **2014**, 1843, 1551.
- [38] V. Sivanathan, A. Hochschild, *Nature protocols* **2013**, 8, 1381.
- [39] P. Q. Nguyen, Z. Botyanszki, P. K. Tay, N. S. Joshi, *Nature communications* **2014**, 5, 4945.
- [40] Z. Botyanszki, P. K. Tay, P. Q. Nguyen, M. G. Nussbaumer, N. S. Joshi, *Biotechnology and bioengineering* **2015**, 112, 2016.
- [41] N.-M. D. Courchesne, Duraj-Thatte, A., Tay, P.K.R., Nguyen, P.Q., and N.S. Joshi. , *ACS Biomaterials Science & Engineering* **2016**, DOI: 10.1021/acsbiomaterials.6b00437.
- [42] U. O. Seker, A. Y. Chen, R. J. Citorik, T. K. Lu, *ACS synthetic biology* **2017**, 6, 266.
- [43] Y. Cao, Y. Feng, M. D. Ryser, K. Zhu, G. Herschlag, C. Cao, K. Marusak, S. Zauscher, L. You, *Nature biotechnology* **2017**, 35, 1087.
- [44] F. Chen, S. V. Wegner, *ACS synthetic biology* **2017**, 6, 2170.
- [45] L. Pu, S. Yang, A. Xia, F. Jin, *ACS synthetic biology* **2018**, 7, 200.
- [46] X. Jin, I. H. Riedel-Kruse, *Proceedings of the National Academy of Sciences of the United States of America* **2018**, 115, 3698.
- [47] H. Salis, A. Tamsir, C. Voigt, *Contrib Microbiol* **2009**, 16, 194.
- [48] C. A. Voigt, *Curr Opin Biotechnol* **2006**, 17, 548.
- [49] S. Yagur-Kroll, C. Lalush, R. Rosen, N. Bachar, Y. Moskovitz, S. Belkin, *Appl Microbiol Biotechnol* **2014**, 98, 885.
- [50] F. Moser, A. Horwitz, J. Chen, W. Lim, C. A. Voigt, *ACS synthetic biology* **2013**, 2, 614.
- [51] T. Waldmingerhaus, J. Kortmann, S. Gesing, F. Narberhaus, *Biol Chem* **2008**, 389, 1319.
- [52] J. Neupert, D. Karcher, R. Bock, *Nucleic acids research* **2008**, 36, e124.
- [53] G. Miesenböck, D. A. De Angelis, J. E. Rothman, *Nature* **1998**, 394, 192.
- [54] W. Weber, N. Link, M. Fussenegger, *Metab Eng* **2006**, 8, 273.
- [55] J. Zhang, N. Sonnenschein, T. P. Pihl, K. R. Pedersen, M. K. Jensen, J. D. Keasling, *ACS synthetic biology* **2016**, 5, 1546.

- [56] L. A. Pola-Lopez, Camas-Anzueto, J.L., Martinez-Antonio, A., Luja-Hidalgo, M.C., Anzueto-Sanchez, G., Ruiz-Valdiviezo, V.M., Grajales-Coutino, R, and J.H. Castanon Gonzalez., *Sensors and Actuators B: Chemical* **2018**, 254, 1061.
- [57] F. Moser, A. Espah Borujeni, A. N. Ghodasara, E. Cameron, Y. Park, C. A. Voigt, *Molecular systems biology* **2018**, 14, e8605.
- [58] A. Tamsir, J. J. Tabor, C. A. Voigt, *Nature* **2011**, 469, 212.
- [59] C. H. Haigler, L. Betancur, M. R. Stiff, J. R. Tuttle, *Front Plant Sci* **2012**, 3, 104.
- [60] D. O. Serra, A. M. Richter, R. Hengge, *Journal of bacteriology* **2013**, 195, 5540.
- [61] D. O. Serra, G. Klauck, R. Hengge, *Environmental microbiology* **2015**, 17, 5073.
- [62] W. Thongsomboon, D. O. Serra, A. Possling, C. Hadjineophytou, R. Hengge, L. Cegelski, *Science* **2018**, 359, 334.
- [63] Z. Saldana, J. Xicohtencatl-Cortes, F. Avelino, A. D. Phillips, J. B. Kaper, J. L. Puente, J. A. Giron, *Environmental microbiology* **2009**, 11, 992.
- [64] M. Rein, V. D. Favrod, C. Hou, T. Khudiyev, A. Stolyarov, J. Cox, C. C. Chung, C. Chhav, M. Ellis, J. Joannopoulos, Y. Fink, *Nature* **2018**, 560, 214.
- [65] X. Liu, T. C. Tang, E. Tham, H. Yuk, S. Lin, T. K. Lu, X. Zhao, *Proceedings of the National Academy of Sciences of the United States of America* **2017**, 114, 2200.
- [66] W. Wang, L. Yao, C. Y. Cheng, T. Zhang, H. Atsumi, L. Wang, G. Wang, O. Anilionyte, H. Steiner, J. Ou, K. Zhou, C. Wawrousek, K. Petrecca, A. M. Belcher, R. Karnik, X. Zhao, D. I. C. Wang, H. Ishii, *Sci Adv* **2017**, 3, e1601984.
- [67] C. Bader, D. Kolb, J. C. Weaver, S. Sharma, A. Hosny, J. Costa, N. Oxman, *Sci Adv* **2018**, 4, eaas8652.
- [68] C. Liu, K. K. Sakimoto, B. C. Colon, P. A. Silver, D. G. Nocera, *Proceedings of the National Academy of Sciences of the United States of America* **2017**, 114, 6450.
- [69] C. Zhong, T. Gurry, A. A. Cheng, J. Downey, Z. Deng, C. M. Stultz, T. K. Lu, *Nature nanotechnology* **2014**, 9, 858.
- [70] E. M. Spiesz, D. T. Schmieden, A. M. Grande, K. Liang, J. Schwiedrzik, F. Natalio, J. Michler, S. J. Garcia, M. E. Aubin-Tam, A. S. Meyer, *Small* **2019**, DOI: 10.1002/sml.201805312e1805312.
- [71] P. Janardhanan, C. M. Mello, B. R. Singh, J. Lou, J. D. Marks, S. Cai, *Talanta* **2013**, 117, 273.
- [72] C. R. Taitt, L. C. Shriver-Lake, M. M. Ngundi, F. S. Ligler, *Sensors (Basel)* **2008**, 8, 8361.
- [73] N. Raab, J. Davis, R. Spokoini-Stern, M. Kopel, E. Banin, I. Bachelet, *Sci Rep* **2017**, 7, 8528.
- [74] J. Dixon, N. Kuldell, *Methods Enzymol* **2011**, 497, 255.

- [75] C. Gupta, Prakash, D., Sneha Gupta., *Journal of Microbiology & Experimentation* **2015**, 2.
- [76] S. Gupta, Bram, E.E., and R. Weiss., *ACS synthetic biology* **2013**, 2, 715.
- [77] N. Saeidi, C. K. Wong, T. M. Lo, H. X. Nguyen, H. Ling, S. S. Leong, C. L. Poh, M. W. Chang, *Molecular systems biology* **2011**, 7, 521.
- [78] L. A. a. M. Y. E.-N. Zacharoff, *Current Opinion in Electrochemistry* **2017**, 4, 182.
- [79] S. M. Strycharz-Glaven, Snider, R.M., Guiseppi-Elie, A., and L.M. Tender, *Energy & Environmental Science* **2011**, 4, 4366.
- [80] K. A. Datsenko, B. L. Wanner, *Proceedings of the National Academy of Sciences of the United States of America* **2000**, 97, 6640.
- [81] D. G. Gibson, G. A. Benders, K. C. Axelrod, J. Zaveri, M. A. Algire, M. Moodie, M. G. Montague, J. C. Venter, H. O. Smith, C. A. Hutchison, 3rd, *Proceedings of the National Academy of Sciences of the United States of America* **2008**, 105, 20404.
- [82] S. M. Richardson, S. J. Wheelan, R. M. Yarrington, J. D. Boeke, *Genome Res* **2006**, 16, 550.

Figures (illustration only -- please use submitted .pdf files for final publication or contact author)

Figure 1

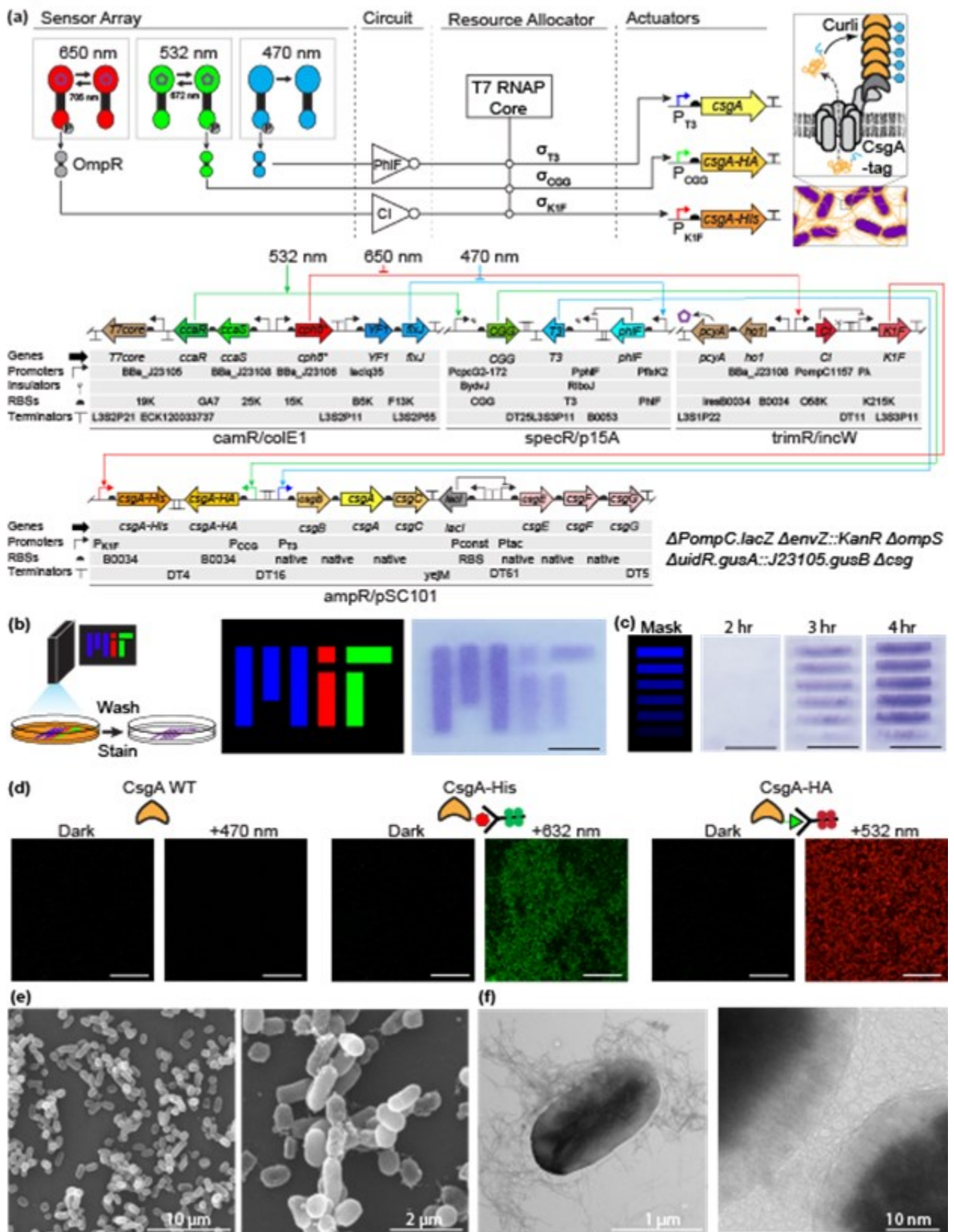


Figure 2

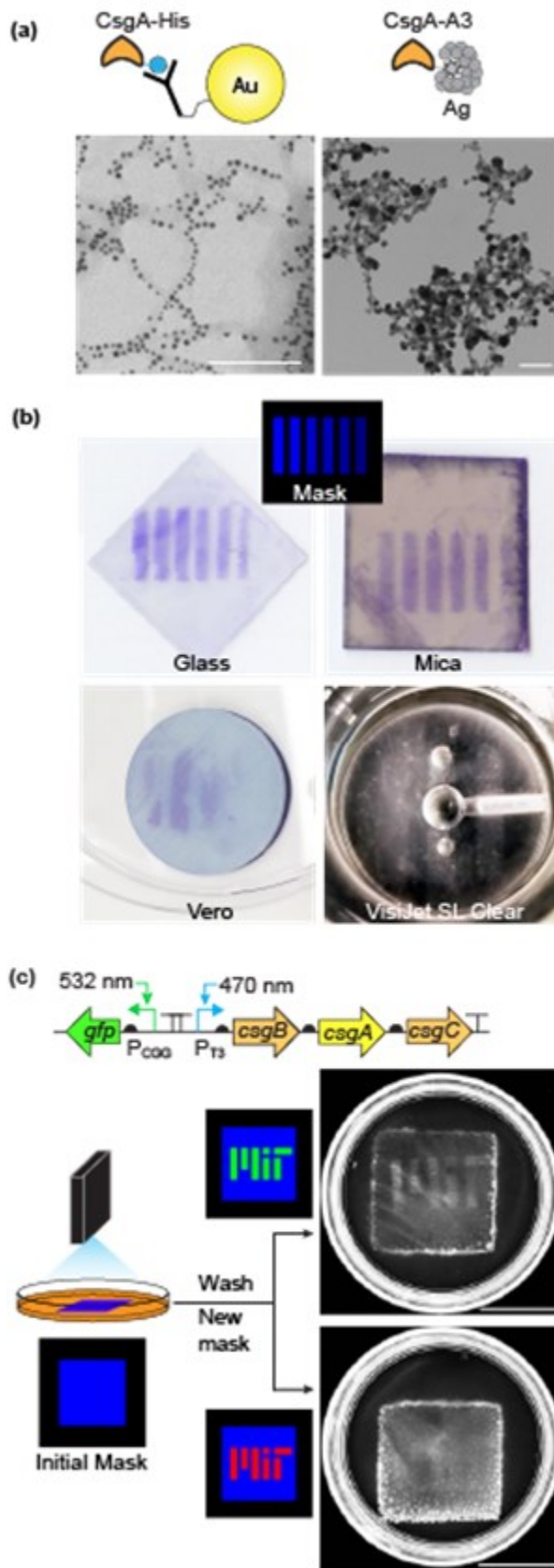
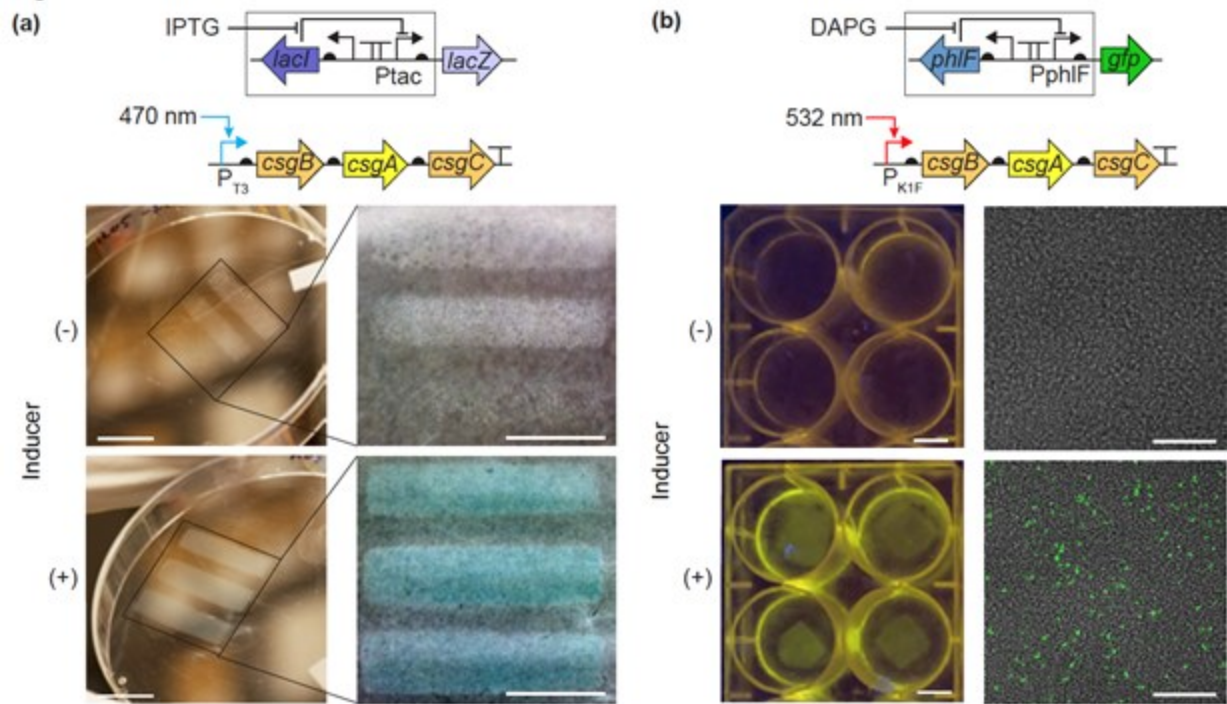
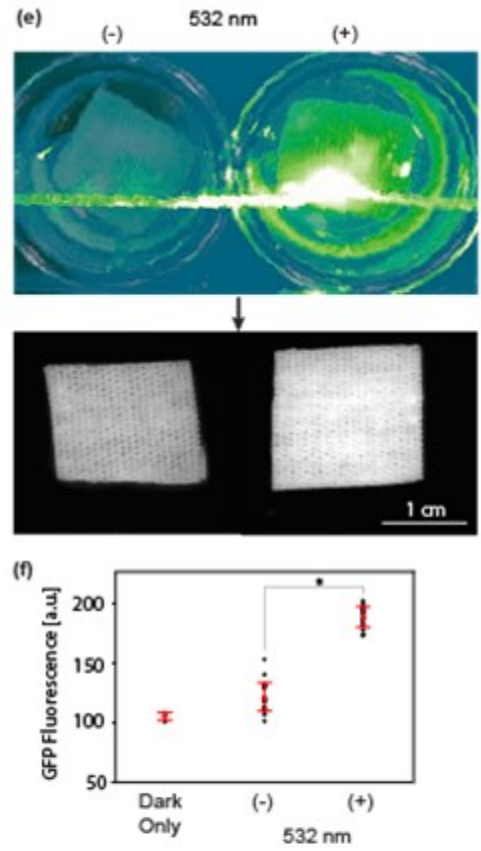
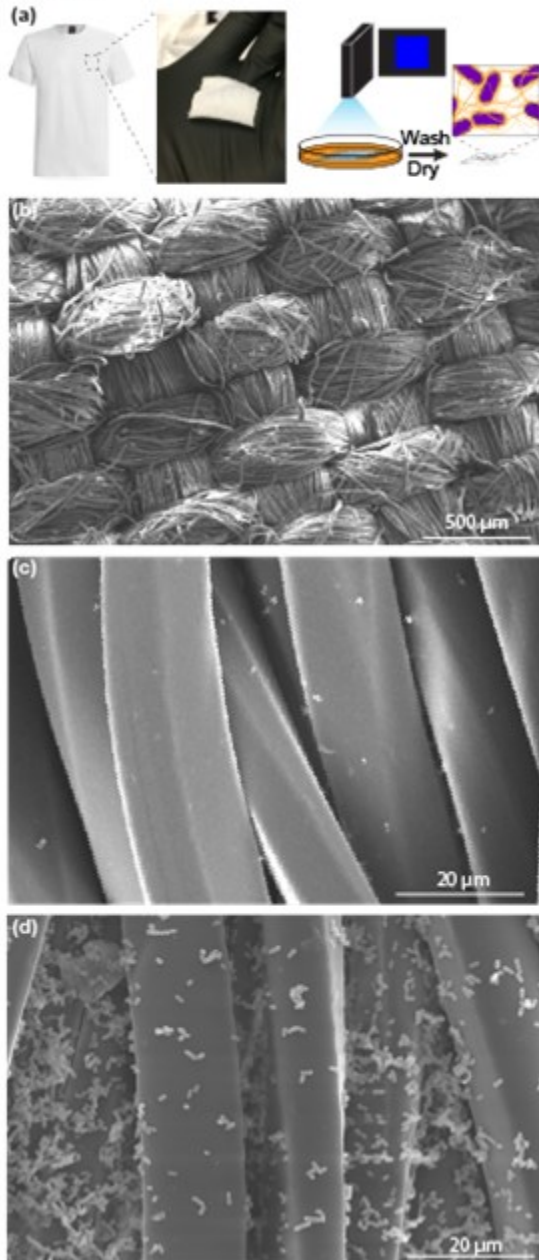


Figure 3



Author Mail

Figure 4



Auth



Figure 5

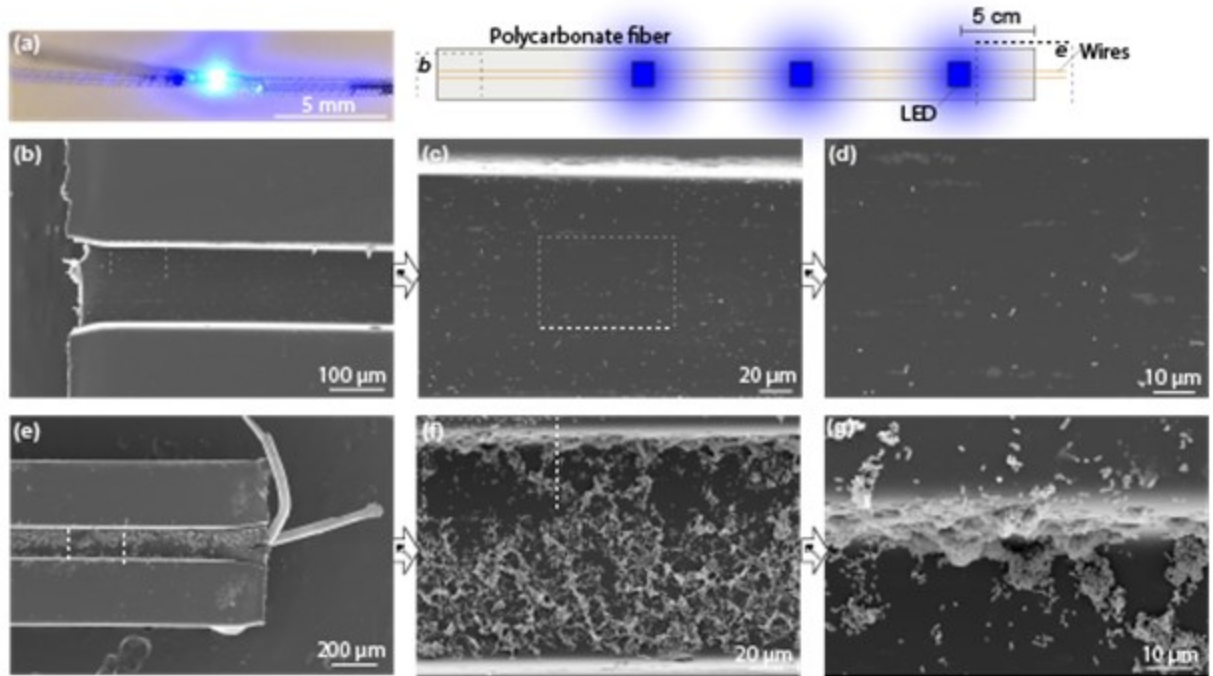


Figure Legends

Author Manuscript

**Figure 1: Optogenetic control of biofilm formation.** (a) Schematic of the optogenetic control system that drives curli biofilm formation. The genetic components of the RGB curli system are shown. The genotype of the host strain is written to the right. The full component sequences and plasmid maps are provided in the Supplemental Information. (b) Schematic of the experimental setup for generating light-induced biofilms. The shown three-color pattern was projected onto a plate containing the RGB curli strain suspended in media. The resulting biofilm was washed and stained with crystal violet. In this strain, blue light induces untagged *csgA*, red light induces His-tagged *csgA*, and green light induces HA-tagged *csgA*. The scale bar is 1 cm. (c) Timed generation of curli biofilm. The scale bars are 1 cm. (d) Each biofilm generated by the 3-color system in part b was simultaneously stained with FITC-conjugated antibody and PE-TxRed-conjugated antibody and then imaged by fluorescence microscopy. The untagged (blue light, 470 nm) *csgA*-WT biofilm is shown on the left and is not expected to bind antibodies, the *csgA*-12xHis (red light, 632 nm) biofilm is shown in the middle, and the *csgA*-HA (green light, 532 nm) biofilm is shown on the right. Dark regions of plate were imaged for comparison. Scale bars are 30  $\mu\text{m}$ . (e) SEM images of the biofilm. (f) TEM images of cells in the biofilm show a fine mesh of nanofibers that aggregate into larger fibers. Data is representative of three independent experiments done on different days.

**Figure 2: Biofilm versatility.** (a) *CsgA*-12xHis curli fibers (left) were labelled with 5 nm diameter nickel nitrilotriacetic acid-conjugated gold particles (NiNTA-AuNPs) and imaged with TEM. NiNTA-AuNPs can be seen as black dots along the fibers. *CsgA*-A3 curli biofilms (right) were washed and then incubated with aqueous  $\text{AgNO}_3$  (150 mM) for 6 hours. The biofilm was then washed with water, scrapped from the plate, and placed on a TEM grid (Methods). The resulting *CsgA*-A3 curli fibers contained variably sized nanoparticles. Scale bars are 100 nm. (b) Blue light-induced WT curli strains can form biofilms on various materials, including glass, mica, and 3D-printed plastics (Vero and VisiJet SL Clear). The VisiJet SL Clear component is unstained and shows visible holes for fixture assembly. (c) Shown is the genetic diagram for a plasmid (pFM1320) encoding a curli output that generates GFP in response to green light. The biofilm is initially formed by projecting a blue square onto the plate. Following washing and addition of fresh media, either a green or red pattern (inset) is projected onto the biofilm for 4 hours. The biofilm is then imaged for GFP production (methods). The red pattern serves as a negative control. Biofilm images were modified in the same layer in Adobe Photoshop to improve visualization. Scale bars in c are 1 cm. Data is representative of three independent experiments done on different days.

**Figure 3: Light-patterned biofilms are robust biosensors. (a)** Shown is the genetic diagram of the Blue Only curli strain that generates  $\beta$ -galactosidase in response to IPTG. Biofilms formed by this strain were exposed to X-Gal and to either no IPTG (top) or 1 mM IPTG (bottom). The close-up images of the biofilm were modified in the same layer in Adobe Photoshop to improve visualization. **(b)** Shown is the genetic diagram of the red-only curli strain that generates GFP in response to DAPG. Biofilms formed by this strain were exposed to either no DAPG (top) or 25  $\mu$ M DAPG (bottom). GFP in the biofilm was imaged on a blue light plate (left) and by fluorescent microscopy (right). Error bars are 1 cm in the left images and 50  $\mu$ m in the right images. Data is representative of three independent experiments done on different days.

**Figure 4: Light-induced adhesion of biofilms to fabric. (a)** Shown is the scheme for inducing biofilm adhesion to cotton fabric. A cotton t-shirt was sectioned into 2x2 cm fabric squares. These squares were immersed in a culture expressing wild-type CsgA in response to blue light and GFP in response to green light. Following exposure to blue light from a projector for 6 hours, the squares were washed, dried, and prepared for SEM. **(b)** SEM of one of the fabric squares at low magnification. **(c)** SEM of a fabric square that was kept in the dark. **(d)** SEM of a fabric square that was exposed to blue light. **(e)** Following blue light exposure and washing, some fabric squares were either placed directly under an LED fiber producing green light (532 nm) or at least 2 cm away. The squares were then imaged for GFP production under blue transillumination. **(f)** The GFP fluorescence of the cotton squares was quantified by software analysis (Methods). The mean and standard deviation of 24 replicates is shown in red. Squares treated with no light (Dark Only) were measured as a control. Bars with an asterisk (\*) indicate a statistically significant difference with p-values less than 0.01, as assessed by a two-variable t-test.

**Figure 5: Light responsive biofilms as living materials. (a)** A picture and diagram of a polycarbonate fiber containing regularly spaced LEDs (20 cm apart) and tungsten wires for conduction. An active fiber was incubated with a culture of a blue-only curli strain, washed, and then sectioned for analysis. Dotted squares and italic letters indicate the part of the wire shown in the corresponding subfigures. **(b-d)** SEM micrographs with increasing magnification (left to right) of a site 5 cm away from the nearest LED **(e-g)** SEM micrographs with increasing magnification (left to right) of a site and a site near an LED. White dotted squares are zoomed areas shown in images to the immediate right. Data is representative of three independent experiments done on different days.

## Table of Contents Figure

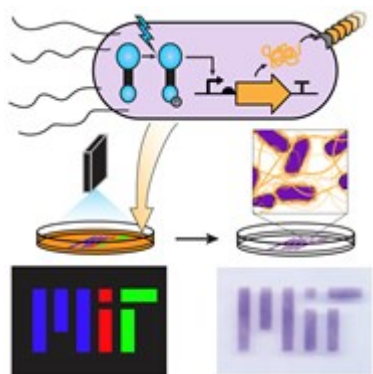


## Table of Contents Description

Bacteria were engineered to generate biofilm material in response to three colors of light. These biofilms could be precisely patterned on diverse materials, including wearable fibers. Cells embedded in the biofilm remained alive and responsive to light and chemical signals. By altering the color of the incident light, the composition of the biofilm material could be finely tuned.

ToC Keyword: Synthetic biology